Utilizing a Fully Digital Approach for Oral Squamous Cell Carcinoma Treatment and Zygomatic Implant-Based Rehabilitation for Maxillary Defects

Shuai Xu, DMD, PhD[1]
Jun Lv, DDS[1]
Yan Zhou, DDS, PhD[2]
Kun Wang, DMD, PhD[2*]

This clinical report details the functional and esthetic rehabilitation of a patient with a severe maxillary defect secondary to subtotal maxillectomy for oral squamous cell carcinoma using a maxillary prosthesis anchored by 4 zygomatic implants. The procedure involved meticulous subtotal maxillectomy and defect repair with zygomatic implant support, incorporating advanced digital surgical methods, including 3D reconstruction, computer-guided surgery, and photogrammetry (Icam4D). A 3D finite element analysis was conducted to assess the method's efficacy in analyzing stress distribution around the zygomatic implants. The patient expressed high satisfaction with the prosthesis's functionality, esthetics, speech, and swallowing capabilities, underscoring the value of zygomatic implant–supported maxillofacial prosthetics. This synergy of advanced planning, surgical precision, and biomechanical analysis marks a significant advancement in maxillofacial prosthetics.

Key Words: ***oral squamous cell carcinoma involving the maxilla, zygomatic implants, digital surgical techniques, 3D finite element analysis, photogrammetry technology***

INTRODUCTION

Oral squamous cell carcinoma involving the maxilla (OSCCM) is uncommon and comprises approximately 6%–7% of all head and neck malignancies.[1,2] Standard OSCCM treatment requires surgery, often complemented by radiotherapy, chemotherapy, and immunotherapy, tailored to tumor stage and lymph node involvement.[3] Complete tumor removal is essential but challenging due to anatomical complexities and limited surgical access with incomplete excision potentially leading to local recurrence and increased patient mortality.[4,5] Aggressive OSCCM treatments result in significant dental and bony structure loss, facial defects, and anatomical changes. En bloc resection for OSCCM can cause maxillary defects, impacting speech, swallowing, nutrition, respiratory health, and facial appearance.[6] Therefore, accurate tumor excision and reconstruction are vital for effective OSCCM management.

Establishing oronasal separation is crucial for enhancing the quality of life in patients with OSCCM and can be accomplished through vascularized osteomyocutaneous flaps or prosthetic devices.[7,8] However, reconstructive surgery is sometimes contraindicated due to patient health conditions or to prevent additional surgical morbidity. Removable maxillary obturator prostheses are key in restoring oral functions, promoting effective swallowing and speech, supporting orbital contents to avoid enophthalmos and diplopia, and enhancing midfacial contour for improved aesthetics.[9] These prostheses are a valuable postoperative reconstruction alternative for OSCCM patients. Nonetheless, fabricating an obturator for OSCCM patients presents difficulties, particularly in the absence of stable dentition and due to variable resection boundaries that may include the hard and soft palate, alveolar ridges, and occasionally the nasal floor, affecting prosthesis retention and stability.[10]

Maxillofacial defect reconstruction after tumor resection is a complex surgical endeavor that demands optimal functional and aesthetic results. Zygomatic implants provide robust retention and support for significant maxillary deficiencies, benefiting from their integration into the zygomatic bone, often less affected by radiation therapy.[11,12] However, the precise placement of these implants is intricate as the absence of clear anatomical landmarks makes the procedure particularly challenging on the defect-affected side due to the extended drill path.[13]

Clinicians face the challenge of achieving precise OSCCM resection and restoration with zygomatic implant support. Advances in virtual surgical planning and 3D printing have improved OSCCM treatment, increasing precision and reliability while allowing for tailored patient care.[14,15] This clinical report describes a meticulous subtotal maxillectomy for OSCCM and the application of a

[1] Department of Oral and Maxillofacial Surgery, The Second Affiliated Hospital, Third Military Medical University (Army Medical University), Chongqing, China.
[2] Department of Prosthodontics and Digital Technology, The Second Affiliated Hospital, Third Military Medical University (Army Medical University), Chongqing, China.
* *Corresponding author,* e-mail: xushuai87@tmmu.edu.cn
https://doi.org/10.1563/aaid-joi-D-24-00115

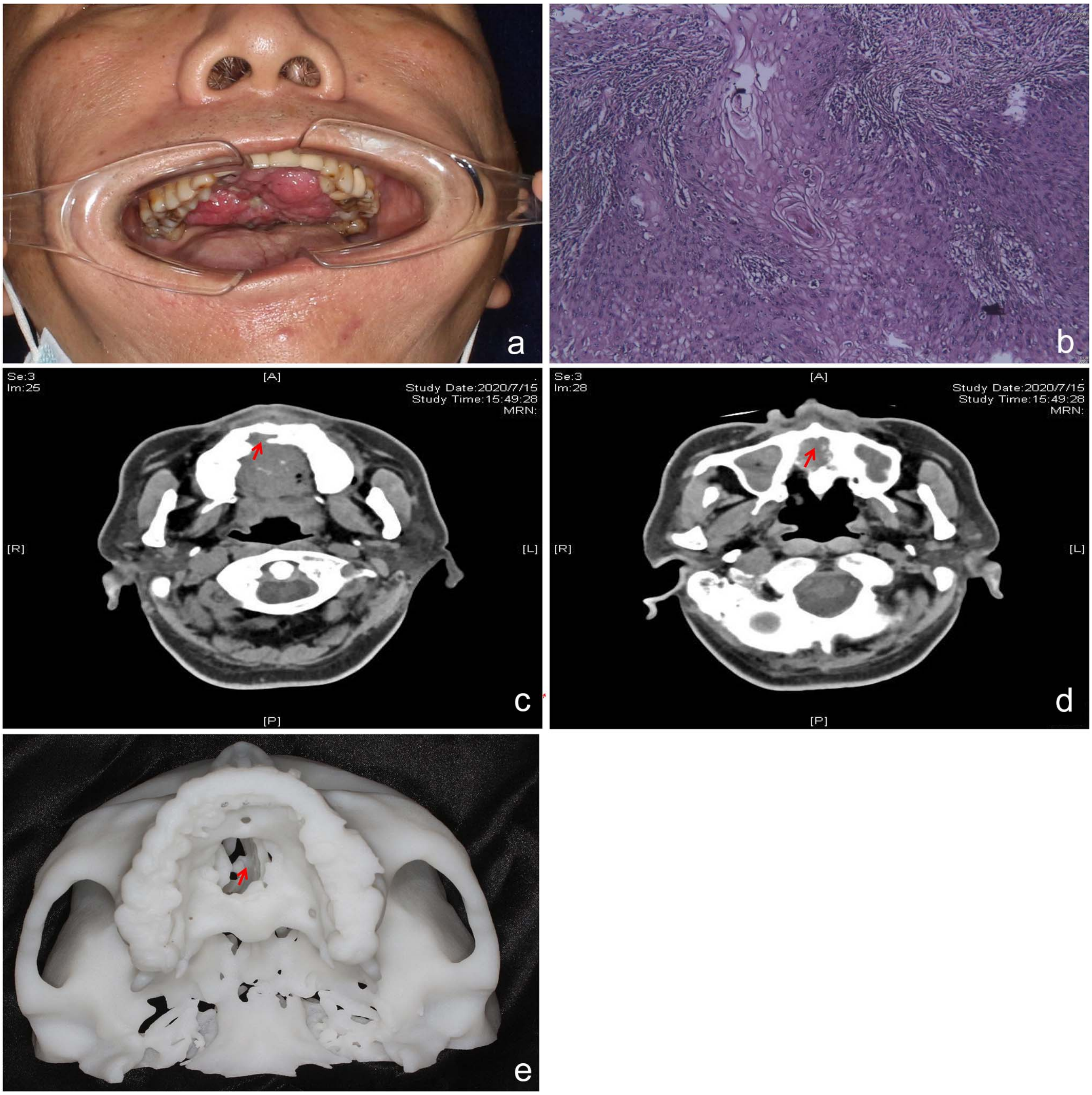

Figure 1. Preoperative assessment of the patient. (a) Oral cavity examination. (b) Pathology report confirming maxillary well-differentiated squamous cell carcinoma. (c through e) Maxillofacial computerized tomography scan and corresponding 3D model highlighting oral squamous cell carcinoma involving the maxilla–induced maxillary damage (indicated by red arrow).

zygomatic implant–supported prosthesis, employing digital techniques including 3D reconstruction, computer-guided surgery, and photogrammetry (Icam4D). Additionally, 3D finite element analysis (FEA) is applied to assess the technique's efficacy and analyze stress patterns around the zygomatic implant.

Clinical Report

A 56-year-old male presented with a painful palate ulcer (Figure 1a) at the Department of Oral and Maxillofacial Surgery and was diagnosed with OSCCM (T4aN0M0, stage IVA, American Joint Committee on Cancer) (Figure 1b). Maxillofacial computerized tomography (CT) scans confirmed OSCCM-induced maxillary damage (Figure 1c and d). To improve surgical accuracy and outcomes, the team employed digital approaches, including virtual surgical planning with a 3D skull model and computer-guided surgery, and designed a digital full-mouth removable denture supported by maxillary implants alongside immediate zygomatic implant placement using a digital guide plate. The plan for permanent restoration is set for 6 months postoperation. The study protocol was approved by the hospital's ethics committee (No. 2020-156-01), and the patient provided informed consent.

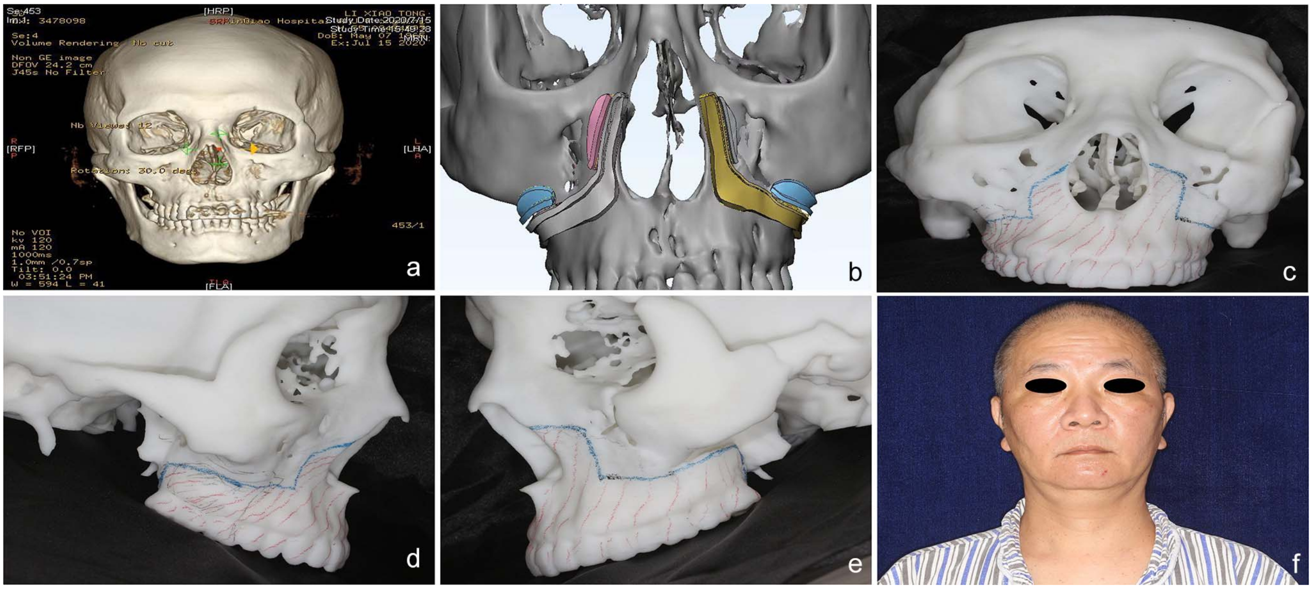

Figure 2. Virtual planning process for maxillary tumor resection. (a) 3D maxillofacial reconstruction. (b) Osteotomy guide with a 2 cm tumor margin. (c through e) Multiview 3D model detailing the osteotomy line (blue arrow denotes the cut line; red marks the excised maxillary segment). (f) Preoperative facial imaging and measurements.

Virtual planning

Preoperatively, virtual surgical planning was conducted alongside generating a 3D skull model and fabricating a reconstruction plate and computer-guided surgery. A head CT scan was acquired with spiral CT equipment (Siemens Sensation 16, Siemens), and the Digital Imaging and Communications in Medicine–formatted data, sliced at 0.625 mm, was processed in Mimics software (version 20.0, Materialise) to create a patient-specific 3D virtual model (Figure 2a). Maxilla resection margins extended 2 cm from the tumor (Figure 2b). The virtual plan was scrutinized in 3 dimensions for optimal outcomes (Figure 2c through e). Digital scans and photographs captured the maxillofacial anatomy and occlusion (Figure 2f). A 3D simulation of the maxilla resection and zygomatic implant reconstruction was completed. Corresponding computer-guided surgery was designed with osteotomy-aligned slots (Figure 3a through d).

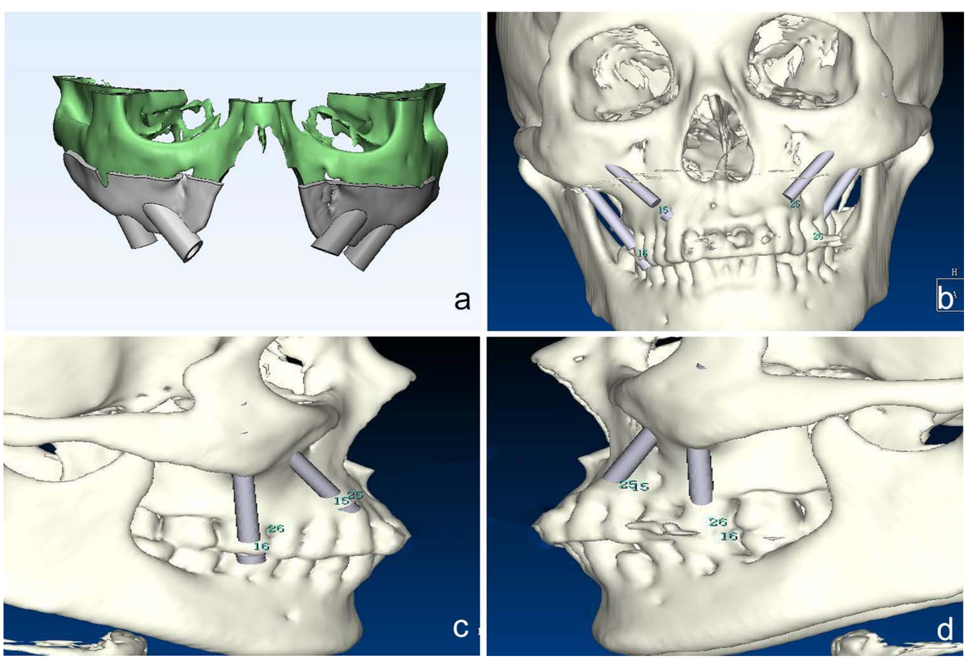

Figure 3. Zygomatic implant guide design. (a) Polyamide 3D-printed guide (gray) displaying bilateral zygomatic implants corresponding to maxillary teeth 15, 16, 25, and 26. (b through d) Frontal and lateral perspectives of the implanted positions.

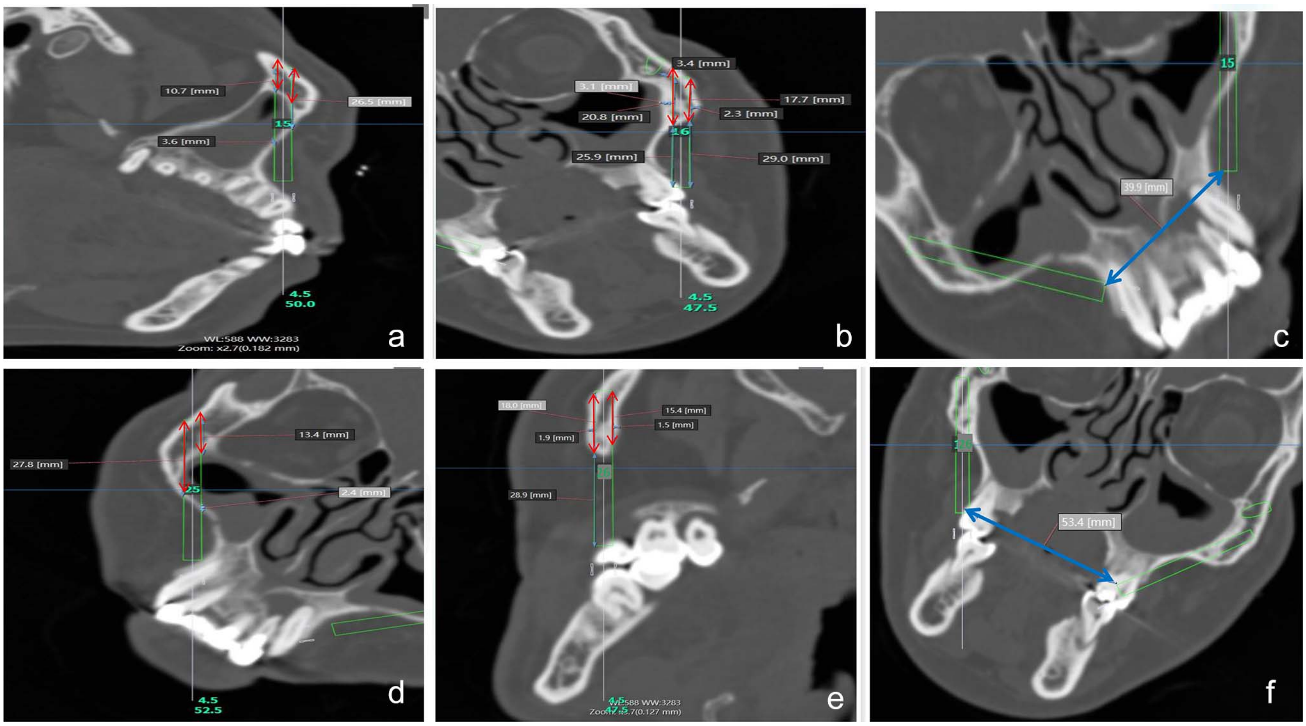

Figure 4. Cone beam computerized tomography (CBCT) assessment for zygomatic implant placement. (a through f) CBCT images delineating the depth and angulation for implant positions 15, 16, 25, and 26 with annotations indicating interimplant distances (blue arrow) and bone-to-implant proximity (red arrow).

Three-dimensional finite element analysis of zygomatic implants for rehabilitation

Zygomatic implant FEA models were constructed (Brånemark System zygomatic implant, Nobel Biocare), adhering to manufacturer specifications. The zygomatic implant length, determined by the distance from the residual maxilla to the jugal point (JU) of the zygomatic bone (45–55 mm), led to the selection of suitable 15 (4.5 × 50 mm), 16 (4.5 × 47.5 mm), 25 (4.5 × 52.5 mm), and 26 (4.5 × 47.5 mm) implants, which were modeled and positioned in the skull for optimal bone contact (Figure 4a through f). The apices of the posterior zygomatic implants were placed close to or slightly protruding through the zygomatic bone's external surface. The prosthesis was designed as a computer-aided design and computer-aided manufacturing milled titanium alloy bar, 10 × 8 mm in size.

All components were integrated into the simulation platform (Ansys Workbench, ANSYS). Engineering data for each material used in the FEA were inputted, assumed homogenous, isotropic, and linearly elastic and were based on the Young modulus and Poisson ratio (Table 1). By threshold processing and image segmentation algorithms, we distinguished between cortical bone (Hounsfield units 700–1500) and cancellous bone (Hounsfield units 100–700). Rigid boundary conditions are imposed at the patient's occipital foramen magnum to preclude rotational movement of the model. The *CONTACT_AUTOMATIC_SINGLE_SURFACE algorithm was utilized between the prosthesis, zygomatic implants, and zygomatic bone to ensure noninterpenetrating contact among the components. A 150 N occlusal force[16,17] was applied to the superstructure's palatal surface (Figure 5a through c) with stress distribution visualized using colored contour bands (Figure 5d). Stress was distributed across the zygomatic implants (Figure 5e) and craniofacial structures (Figure 5f), peaking at the implant-abutment connection (100.15–78.05 Mpa, Figure 5g) and minimal at the prosthesis (4.92–3.12 Mpa, Figure 5h). The designed obturator prostheses ensured stability on both zygomatic implants and the remaining maxillary structures.

After the virtual surgical plan was approved, stereo models for reconstruction, maxillary osteotomy, zygomatic implant guidance, and templates were created and converted into STL files for 3D printing using a rapid prototyping machine (Wiiboox, JOC) and clear heat-polymerized acrylic resin (Figure 6a and b). The resulting computer-guided surgery, skull model, and plates were then prepared for sterilization.

Surgical techniques

The surgery began with maxillary exposure, followed by attaching the maxillary osteotomy guide to facilitate the planned resection

Table 1

Material properties used in finite element analysis

Material	Young Modulus E(MPa)	Poisson Ratio
Cortical bone	13 400	0.30
Cancellous bone	1 000	0.30
Zygomatic bone	11 653	0.30
Titanium alloy	110 000	0.33
Prosthesis	2 700	0.35

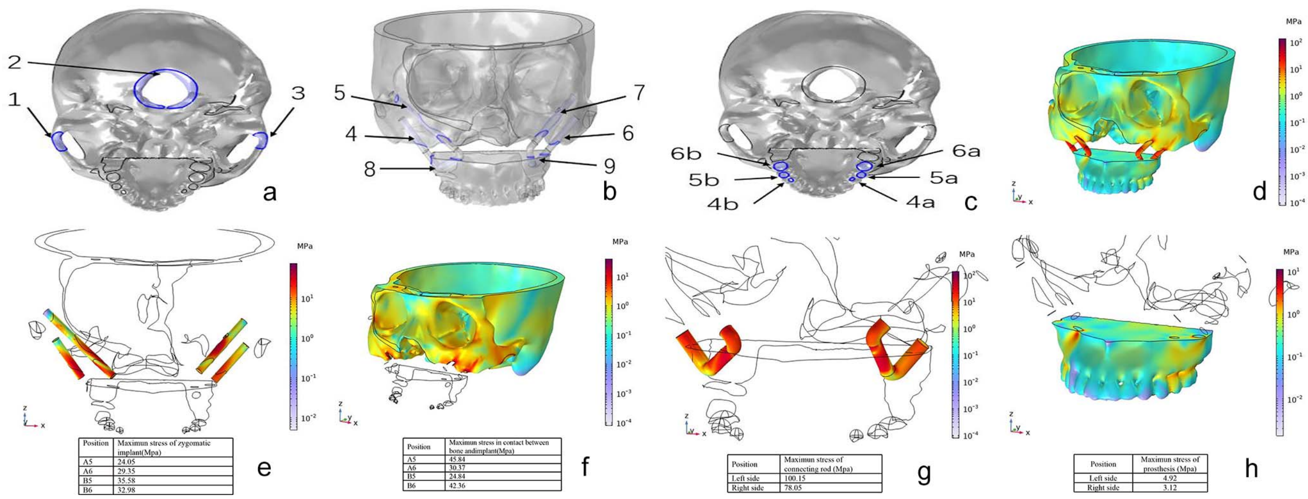

Figure 5. 3D finite element analysis of zygomatic implants in rehabilitation. (a) Imposed constraints at regions 1–3. (b) Contact interfaces between zygomatic implants and the maxilla at sites 4–7 and between implants and prosthesis at sites 8 and 9. (c) Distribution of 90N vertical loads at contact points 4a, 5a, 4b, and 5b; 60N loads at 6a and 6b. (d) Comprehensive Mises stress distribution. (e) Mises stress representation of implant-bone interaction for 4 zygomatic implants. (f) Stress mapping within the bone adjacent to the 4 implants. (g) Stress visualization in the connecting bar with prosthetic contact at 4 implants. (h) Stress pattern within the prosthesis engaging 4 implants, accompanying table details peak stress values (Mpa) at respective locations.

(Figure 7a through c). The resection ensured tumor-free soft tissue margins, confirmed by frozen section analysis. A bilateral neck dissection was conducted, and no metastasis was found in the specimens. The zygomatic implant plate was then fixed to the residual maxilla, addressing the defect left by the resection. Zygomatic implants were accurately placed according to the preoperative plan and computer-guided surgery (Figure 7d) with Brånemark System implants installed at positions 15, 16, 25, and 26 (Figure 7e through g), using a 15 N.cm torque. These implants were secured into the zygomatic bone, passing through the maxillary sinus frontal wall with the implant head visible on the buccal side of the sinus wall. Guided bone regeneration (GBR) was used to cover the exposed implant surfaces with cortical bone grafts from Bio-Oss (Geistlisch, Switzerland) on the buccal side of the implants (Figure 7e through h), and a resorbable collagen membrane Bio-Gide (Geistlich, Switzerland) was placed over the surface. The designed digital full-mouth removable denture was not immediately placed during the surgical procedure. The primary reason was the initial instability of the zygomatic implants and, second, to reduce the duration of the surgery and avoid unnecessary stress on the zygomatic implants during the healing process. Post-subtotal maxillectomy and zygomatic implantation, iodoform gauze is utilized for wound compression to mitigate bleeding. The dressing is subsequently excised 1 week postoperatively (Figure 7h). Postoperative cone beam CT (CBCT) analysis indicates that the zygomatic implants are optimally positioned with minimal distances to the orbital floor at 3.61 mm for implant 15 and 2.52 mm for implant 25 (Figure 7i and j). The precise alignment adheres to the preoperative 3D plan, preserving the integrity of the maxillofacial anatomical structures. Six weeks later, the patient received adjuvant radiotherapy (54 Gy in 30 sessions at 1.8 Gy per session) and chemotherapy (Cisplatin 20 mg).

Fit of the implant retained obturator prosthesis

At 6 months postsurgery, the patient exhibited stable vital signs with no evidence of tumor recurrence or metastasis. The intraoral incision has healed satisfactorily, and a modest amount of hyperplastic mucosa is present surrounding the implant site (Figure 8a). Six months after surgery, the patient was examined with a CBCT

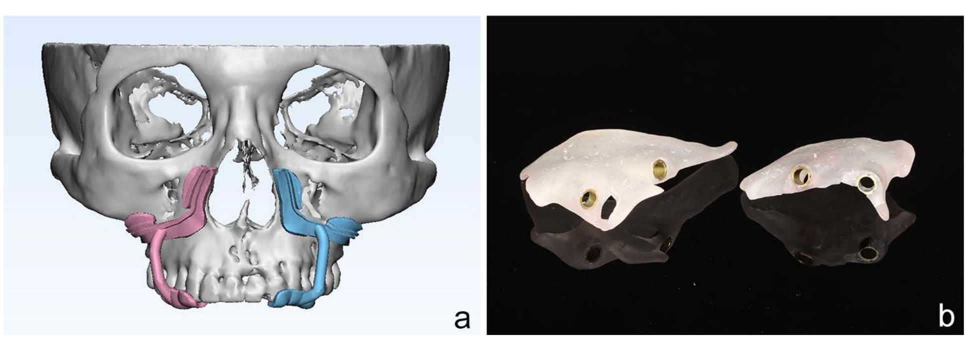

Figure 6. Computer-guided surgery for osteotomy and implantation. (a) Virtual rendering of the maxillary osteotomy guide. (b) 3D-printed zygomatic implant surgical template.

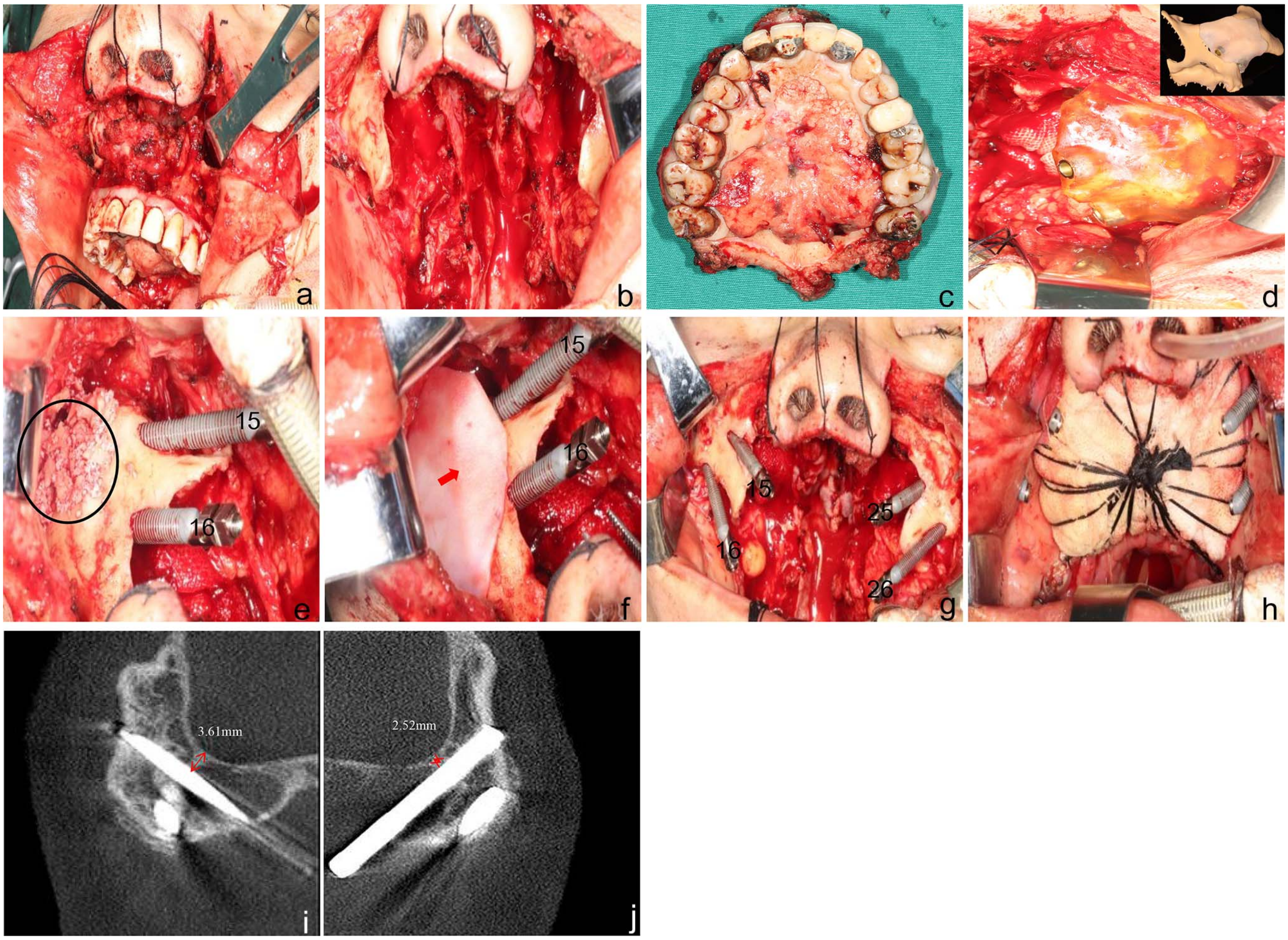

Figure 7. Surgical procedure summary. (a through c) Maxillary tumor resection facilitated by a custom surgical guide. (d) Teeth 25 and 26's drill guide is fixed at zygomatic and premaxillary sites. The upper right photo shows the guide's placement on the zygomatic model; the lower right shows its intraoperative position. (e through g) Application of guided bone regeneration for the exposed surfaces of zygomatic implants. (h) Use of iodoform gauze for wound compression and dressing. (i and j) Postoperative cone beam computerized tomography analysis confirms optimal positioning of the zygomatic implants with minimal distances to the orbital floor of 3.61 mm for implant 15 and 2.52 mm for implant 25, aligning with the guided protocol. The black circular marker indicates the bone graft material, and the red arrows denote the resorbable collagen membrane.

scan, confirming good osseointegration of the zygomatic implants (Figure 8b and c). A CBCT examination was conducted on the patient, revealing robust osseointegration of the zygomatic implants. Additionally, the imaging demonstrated the presence of neo-ossification within the region of the zygomatic implant GBR, indicative of successful bone regeneration (Figure 8d). A digital impression was subsequently taken using the ICam4D photogrammetry system (Imetric4D Imaging Sàrl) (Figure 8e and f), which involved an intraoral scanner for soft tissue STL data and an external scanner for capturing zygomatic implant position and orientation. This data was merged into digital design software, and a 10 × 8 mm milled titanium alloy bar was crafted to connect with multiunit abutments, following the preoperative plan.

A digital occlusal frame was used to design an integrated upper bracket and wax shape, informed by preoperative jaw position records. The occlusal surface morphology and relationship from the preoperative scan guided adjustments for optimal occlusion and function, aiming for balance articulation, early contact and interference prevention, and proper tooth coverage. The prosthesis design considered principles of complete denture restoration, focusing on balance articulation, reduced posterior tooth size, decreased apex inclination, and deepened occlusal sockets for esthetic coverage of anterior teeth. The denture's arch was customized to fit the patient's jaw and implant abutment positions. Trial fitting involved digital preparation of the removable obturator, ensuring proper fit and occlusal efficacy. The fabrication of the zygomatic implant–supported prosthesis was then finalized (Figure 8g and h).

Postoperative assessment

Six months after surgery, a postoperative CT scan confirmed excellent osseointegration of the zygomatic implants, consistent with the initial virtual plans (Figure 8b through d). Over a 3-year follow-up, the patient remained disease-free with no signs of lesion recurrence. After reconstruction, the patient enjoyed clear speech, effective swallowing, and a regular diet (Figure 9a through f). The implants and prosthesis have been stable and complication-free for 3 years postfunctional loading. Postoperative

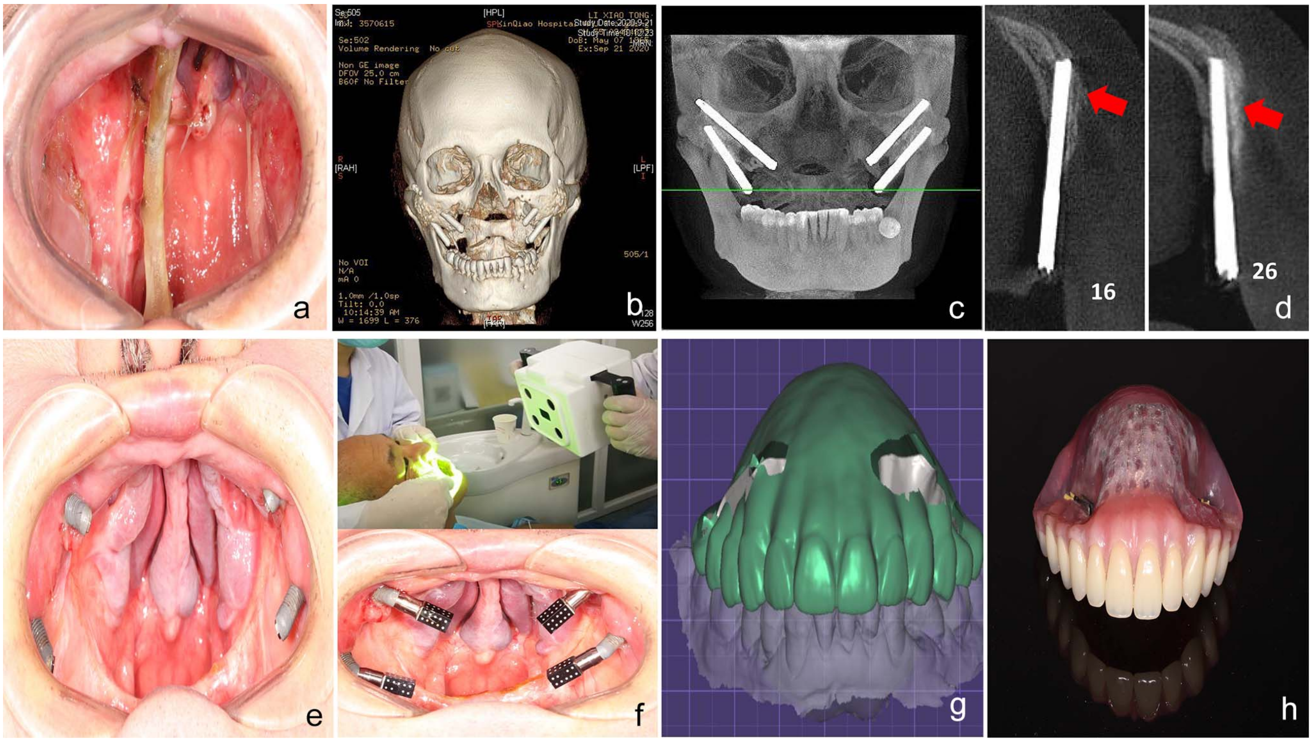

Figure 8. Design and fabrication of zygomatic implant–supported restorations. (a) The 6-month postoperative intraoral assessment demonstrated satisfactory wound healing and mild hyperplasia of the mucosa surrounding the zygomatic implants. (b and c) Postimplantation cone beam computerized tomography (CBCT) imaging at 6 months. (d) Concurrent CBCT imaging confirmed robust osseointegration and the presence of new bone formation as indicated by the red arrow. (e and f) Digital impressions with a photogrammetry system involves scanning bodies on replica abutments before digitization. (e) Setup of the ICambodies scanning cap; (f) Acquisition of implant position data using the ICam4D intraoral scanner. (g and h) Computer-aided design and manufacture of a complete overdenture with implant and bar-clip mechanisms.

CBCT analysis at the 3-year mark revealed deviation angles of zygomatic implants, which is crucial for evaluating the accuracy of implant positioning. The comparison with the preoperative zygomatic implant guide indicated a maximum deviation of 5.78° for implant 16 and a minimum of 0.69° for implant 25, underscoring the precision of the surgical placement (Figure 10a). Both the patient and surgeons evaluated postoperative esthetics, speech, and masticatory function, noting a near-preoperative midfacial appearance and a 3.5-cm mouth opening range (Figure 10b, Table 2). Serial CBCT scans performed on the day of surgery and at 6 months, 1 year, and 3 years postoperatively demonstrated stable graft integration without notable resorption (Figure 10c). The patient reported high satisfaction with the functional and esthetic results of the prosthesis.

Discussion

This study shows that digital surgical methods are effective for predictable OSCCM resection, zygomatic implant placement, and prosthetic restoration in postmaxillectomy OSCCM patients, potentially reducing surgical and prosthetic complications.

Restoring oral function in patients with OSCCM is intricate. Negative margin resection in OSCCM is especially challenging, requiring detailed knowledge of the tumor's extent.[18,19] This study utilized computer-aided planning and rapid prototyping to map the maxillofacial area's anatomy and pathology accurately, enhancing presurgical planning for precise resection and defect reconstruction while safeguarding critical structures. The choice of postmaxillectomy rehabilitation, influenced by defect size, patient factors, and comorbidities, aims to restore maxillary support, esthetics, and oral function. Common approaches include vascularized bony flaps and dental implants. However, these may not be ideal for older patients or those facing postoperative radiotherapy due to the risk of surgical wound complications.[7] An implant-retained obturator prosthesis, removable for inspection and management of complications,[20] was selected for this case. Therefore, in this case, the treatment choice was a zygomatic implant–supported, full-mouth removable denture as it allowed for the preservation of bilateral zygomatic bones during cancer ablative surgery.

The complex nature of head and neck surgery, particularly in maxillary and midface tumor management, extends beyond disease control to include optimizing reconstruction and rehabilitation strategies.[21] Traditional maxillectomy techniques, heavily dependent on a surgeon's expertise, have yielded inconsistent outcomes. Digital surgery has revolutionized this field, allowing for precise virtual planning that can be accurately executed with computer-guided surgery.[22] Preoperative digital models crafted from photocured polyacrylic resins offer significant advantages, enabling comprehensive planning and testing of resection and reconstruction scenarios, ensuring patient safety, and reducing procedural time.[23,24] In the case of OSCCM treatment, virtual

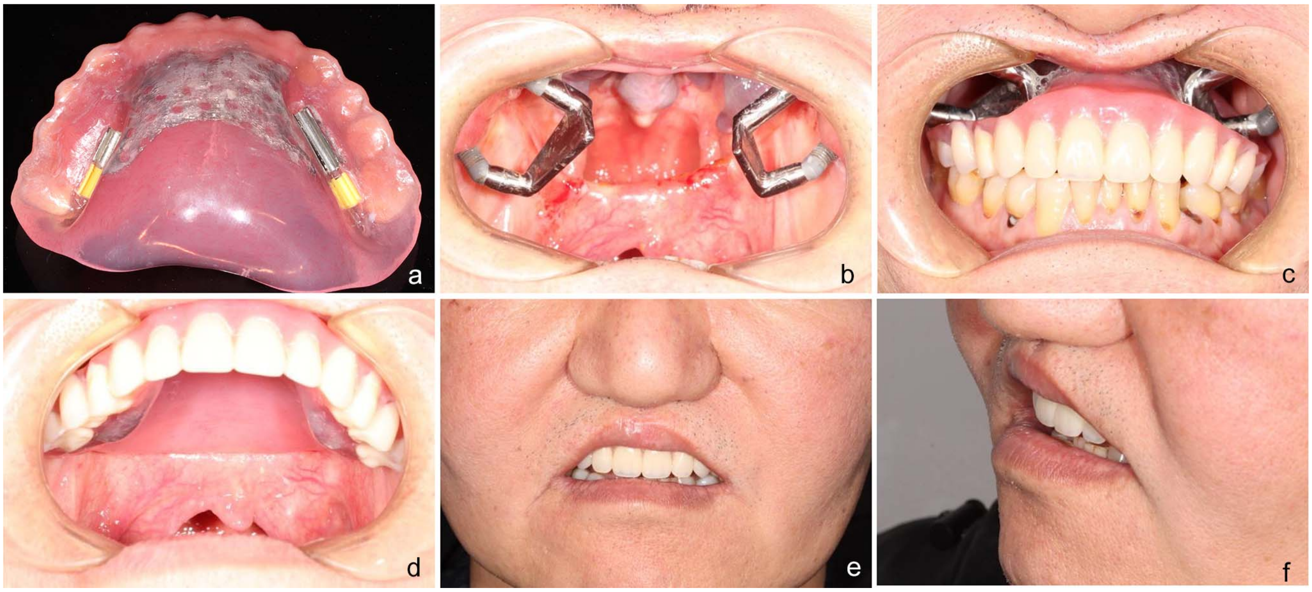

Figure 9. Postoperative outcomes of zygomatic implant–supported oral rehabilitation for maxillary reconstruction. (a) Complete denture integrated with zygomatic implant bar attachment. (b) Implant bar connector for attachment stability. (c) Intraoral view depicting optimal prosthetic occlusion. (d) Intraoral view exhibiting competent palatopharyngeal closure. (e and f) Extraoral frontal and lateral views of the prosthesis, including the restored upper lip contour.

planning and 3D printing have increased accuracy and predictability, facilitating patient-specific resection solutions.

En bloc resections for extensive OSCCM often compromise the separation between oroantral and oronasal compartments, creating speech, eating, swallowing, and breathing difficulties.[25] Postsurgery, implant-supported prostheses are usually required, but the scarcity of adequate bone for implantation poses a challenge. Surgeons may opt for distant bone structures, such as the zygomatic bone

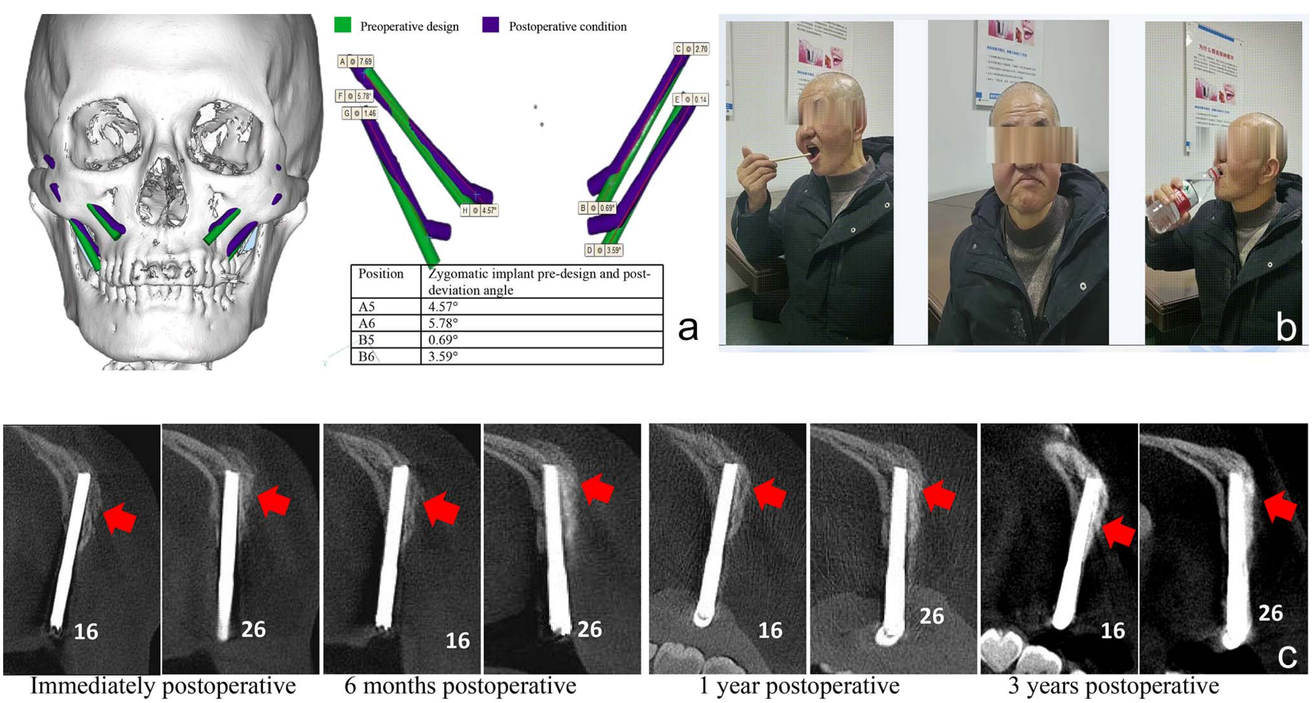

Figure 10. Precision in zygomatic implant placement and postoperative outcomes: aesthetic, functional, and integration assessments over 3 years. (a) Comparison of angular deviations between the preoperative zygomatic implant guide (green) and the 3-year postimplantation placement (purple). (b) Evaluation of postoperative facial esthetics, speech, and masticatory and swallowing functions in the patient. (c) Serial cone beam computerized tomography scans were performed on the day of surgery and at 6 months, 1 year, and 3 years postoperatively to examine the stability of the zygomatic implant–supported bone grafts (red arrows).

TABLE 2

Postoperative functional assessment of the zygomatic implant–supported removable partial denture for the patient

Assessment project	Postoperative Time (months)	6	12	18	24	30	36
Masticatory efficiency: Peanut weighing experiment	Masticatory efficiency	95.50%	93.10%	94.30%	92.10%	93.16%	94.20%
Phonetic test: Phonetically balanced syllable table	Phonetic score	70.7	69.3	72	70.7	71.35	71.62
Swallowing function	Assessment outcome*	Excellent	Excellent	Excellent	Excellent	Excellent	Excellent

*Assessment outcome: Excellent: 1-time 30 ml intake; good: twice within 5 seconds; fair: completed with choking; poor: multiple attempts with choking; nonfunctional: inability to drink.

or the palatopterygoid fusion zone, to secure the prosthesis. The zygomatic bone, less likely to be irradiated, offers a favorable anchorage site, especially beneficial when postoperative radiotherapy is anticipated.[10,11,26] Zygomatic implants postmaxillectomy can enhance prosthetic support, and studies have underscored the benefits of prosthodontic rehabilitation after ablative surgery.[26] However, the precise placement of zygomatic implants without anatomical guides is complex, particularly when dealing with the long drill path and absence of the maxilla on the defect side. Implants may not be fully seated in hard tissue due to the resection cavities, and incorrect placement could lead to complications, such as uncontrolled bleeding, orbital damage, maxillary sinus perforation, and orbitozygomatic complex fractures.[26] Inaccurate implant positioning and angulation may also cause prosthetic misalignment. This study employed 3D reconstruction and surgical guidance to place 4 zygomatic implants immediately after OSCCM resection. In oral implantology, angular deviations of less than 10° are deemed acceptable for achieving osseointegration and functional restoration.[27] In this case report, all deviations measured fell within this threshold. To fully leverage the limited residual zygomatic bone and ensure implant stability, we positioned the implant apices close to or slightly beyond the bone's external surface. This placement aligns with biomechanical principles, optimizing implant anchorage and load bearing by proximity to cortical bone and promoting favorable stress distribution for implant longevity. The 3-year postoperative assessment revealed sustained stability of the zygomatic implants, underscoring the significance of accurate placement in facilitating osseointegration, minimizing complications, and enhancing patient satisfaction. The findings indicate that digital surgical planning improves accuracy and predictability, enabling customized zygomatic implant–supported repair for post-OSCCM resection patients.

This case study utilized 3D FEA to assess the viability of zygomatic implant–supported dentures, specifically by examining stress distribution around the implants to evaluate their capacity to support bite forces.[28] Understanding stress and load transfer at the implant-bone interface is crucial for the success of the implants. There is a risk that overloading these implants could fail. Whereas clinical evaluation is necessary to understand the biomechanical behavior of implants, it is not feasible to directly assess every component due to structural complexity, ethical considerations, and the prolonged duration of studies. As it enables the analysis of various complex geometries and implant configurations, FEA is beneficial in these situations.[29] In this study, the implant surface was assumed to be fully in contact with the bone with uniform forces and displacements at the interface. The analysis revealed maximum von Mises stresses and total deformation, visualized on a colored scale. Stresses under a 150N force ranged from 14.05 MPa to 35.58 MPa, consistent with previous research.[16,17,29] These stresses were effectively distributed across facial buttresses, prostheses, implants, and dentate skulls. The study concluded that 4 zygomatic implants could support a bite force effectively as demonstrated through FEA. Whereas the FEA provided valuable insights into the biomechanical behavior of the implant-supported prosthesis, it is essential to consider the study's limitations. The static load application may not capture the full spectrum of functional loads.

Additionally, the assumption of complete osseointegration might reflect something other than the variability observed in clinical practice. The observed stress concentrations at the implant-abutment connection over the implants suggest further studies exploring the long-term effects of such distributions. The postoperative outcomes demonstrate the patient's enhanced mastication, ability to chew peanuts without difficulty, improved articulation, and the absence of dysphagia during liquid intake, all indicative of optimal prosthetic function. These findings suggest a successful osseointegration with the zygomatic bone and patient adaptation to the prosthesis. This approach exhibits marked superiority over traditional prosthetic augmentation for maxillary reconstruction.

Trismus, xerostomia, and mucositis frequently complicate OSCCM treatments, leading to fibrosis that restricts mouth opening and hinders prosthodontic processes. This difficulty is compounded for dentists taking impressions and patients inserting obturators.[30] However, digital impression techniques such as intraoral scanning and photogrammetry, which use photographs for precise measurements, can effectively address these challenges. Photogrammetry is especially beneficial for complex cases involving multiple implants, significant distances between them, and varied angulations. The ICam4D photogrammetry system is renowned for its precision in long-span implant-supported restorations.[31] It utilizes photographic data to create director vectors to accurately determine the relative positions of scan bodies, which can improve accuracy without the need for picture overlap. This system is operated extraorally, reducing the influence of saliva and blood and limiting mouth opening on precision.[32] In this instance, the combination of intraoral scanning and photogrammetry technology effectively overcame postoperative mouth opening restrictions and achieved successful maxillofacial reconstruction and occlusion.

CONCLUSIONS

Our clinical report introduces a groundbreaking protocol for severe maxillary defect rehabilitation post-OSCCM, tackling a complex reconstruction challenge. We've optimized zygomatic implant placement for biomechanical success by employing cutting-edge digital surgery and FEA. Icam4D's precision captured the patient's anatomy, enabling a customized prosthesis. The patient's functionality, esthetics, speech, and swallowing satisfaction highlight our method's effectiveness. This synergy of advanced planning, surgical precision, and biomechanical analysis marks a significant advancement in maxillofacial prosthetics.

Acknowledgments

This work was supported by grants from the Part 73: China Postdoctoral Science Foundation of China (No. 2023M734255), the Program of State Key Laboratory of Oral and Maxillofacial Reconstruction and Regeneration (No. 2021KB02), and the Youth Training Program of the Second Affiliated Hospital of the Army Medical University (No. 2022YQB048).

Note

There are no conflicts of interest in this study. The participants consented to the study according to the declaration of Helsinki and granted written approval for the publication and use of their photographs in various forms.

References

1. Tan Y, Wang Z, Xu M, et al. Oral squamous cell carcinomas: state of the field and emerging directions. *Int J Oral Sci*. 2023;15:44.
2. Farhood Z, Simpson M, Ward GM, Walker RJ, Osazuwa-Peters N. Does anatomic subsite influence oral cavity cancer mortality? A SEER database analysis. *Laryngoscope*. 2019;129:1400–1406.
3. Johnson DE, Burtness B, Leemans CR, Lui VWY, Bauman JE, Grandis JR. Head and neck squamous cell carcinoma. *Nat Rev Dis Primers*. 2020;6:92.
4. Slieker FJB, de Bree R, Van Cann EM. Oral squamous cell carcinoma involving the maxillae: factors affecting local recurrence and the value of salvage treatment for overall survival. *Head Neck*. 2020;42:1821–1828.
5. Slieker FJB, Rombout DAA, de Bree R, Van Cann EM. Local recurrence and survival after treatment of oral squamous cell carcinoma of the maxilla: a systematic review and meta-analysis. *Oral Surg Oral Med Oral Pathol Oral Radiol.* 2022;133:626–638.
6. Rieger J, Wolfaardt J, Seikaly H, Jha N. Speech outcomes in patients rehabilitated with maxillary obturator prostheses after maxillectomy: a prospective study. *Int J Prosthodont*. 2002;15:139–144.
7. Massarelli O, Gobbi R, Biglio A, Soma D, Tullio A. Chimeric lateral supramalleolar artery perforator fibula free flap in the reconstruction of composite head and neck defects. *Plast Reconstr Surg*. 2014;133:130–136.
8. Wang YY, Fan S, Zhang HQ, Lin ZY, Ye JT, Li JS. Virtual surgical planning in precise maxillary reconstruction with vascularized fibular graft after tumor ablation. *J Oral Maxillofac Surg*. 2016;74:1255–1264.
9. King E, Abbott C, Dovgalski L, Owens J. Orofacial rehabilitation with zygomatic implants: CAD-CAM bar and magnets for patients with nasal cancer after rhinectomy and partial maxillectomy. *J Prosthet Dent*. 2017;117:806–810.
10. Kreissl ME, Heydecke G, Metzger MC, Schoen R. Zygoma implant-supported prosthetic rehabilitation after partial maxillectomy using surgical navigation: a clinical report. *J Prosthet Dent*. 2007;97:121–128.
11. Aparicio C, Manresa C, Francisco K, et al. Zygomatic implants: indications, techniques and outcomes, and the zygomatic success code. *Periodontol 2000*. 2014;66:41–58.
12. Gaur V, Patel K, Palka L. An implant-supported prosthetic rehabilitation of a patient with a bilateral subtotal maxillectomy defect secondary to rhino-orbital-cerebral mucormycosis: a clinical report of a graftless approach. *J Prosthet Dent*. 2022;128:101–106.
13. Noh K, Pae A, Lee JW, Kwon YD. Fabricating a tooth- and implant-supported maxillary obturator for a patient after maxillectomy with computer-guided surgery and CAD/CAM technology: a clinical report. *J Prosthet Dent*. 2016;115:637–642.
14. Han L, Zhang X, Guo Z, Long J. Application of optimized digital surgical guides in mandibular resection and reconstruction with vascularized fibula flaps: two case reports. *Medicine (Baltimore)*. 2020;99:e21942.
15. Nyirjesy SC, Heller M, von Windheim N, et al. The role of computer aided design/computer assisted manufacturing (CAD/CAM) and 3-dimensional printing in head and neck oncologic surgery: a review and future directions. *Oral Oncol*. 2022;132:105976.
16. Miyamoto S, Ujigawa K, Kizu Y, Tonogi M, Yamane GY. Biomechanical three-dimensional finite-element analysis of maxillary prostheses with implants. Design of number and position of implants for maxillary prostheses after hemi-maxillectomy. *Int J Oral Maxillofac Surg*. 2010;39:1120–1126.
17. Ujigawa K, Kato Y, Kizu Y, Tonogi M, Yamane GY. Three-dimensional finite elemental analysis of zygomatic implants in craniofacial structures. *Int J Oral Maxillofac Surg*. 2007;36:620–625.
18. Ooms M, Ponke L, Winnand P, et al. Predictive factors and repetition numbers for intraoperative additional resection of initially involved soft tissue resection margins in oral squamous cell carcinoma: a retrospective study. *World J Surg Oncol*. 2023;21:308.
19. Slieker FJB, Dankbaar JW, de Bree R, Van Cann EM. Detecting bone invasion of the maxilla by oral squamous cell carcinoma: diagnostic accuracy of preoperative computed tomography versus magnetic resonance imaging. *J Oral Maxillofac Surg*. 2020;78:1645–1652.
20. Gundogdu M, Cansever S, Karaavcı MS, Ertas U. Implant-supported prosthetic rehabilitation of a patient with squamous cell carcinoma: a case report. *J Oral Implantol*. 2022;48:215–219.
21. Vosselman N, Alberga J, Witjes MHJ, et al. Prosthodontic rehabilitation of head and neck cancer patients—challenges and new developments. *Oral Dis*. 2021;27:64–72.
22. Dawood A, Tanner S, Hutchison I. Computer guided surgery for implant placement and dental rehabilitation in a patient undergoing sub-total mandibulectomy and microvascular free flap reconstruction. *J Oral Implantol*. 2013;39: 497–502.
23. Vosselman N, Glas HH, Merema BJ, et al. Three-dimensional guided zygomatic implant placement after maxillectomy. *J Pers Med*. 2022;12.
24. Tejo-Otero A, Buj-Corral I, Fenollosa-Artés F. 3D printing in medicine for preoperative surgical planning: a review. *Ann Biomed Eng*. 2020;48:536–555.
25. Yamamoto Y. Mid-facial reconstruction after maxillectomy. *Int J Clin Oncol*. 2005;10:218–222.
26. Hackett S, El-Wazani B, Butterworth C. Zygomatic implant-based rehabilitation for patients with maxillary and mid-facial oncology defects: a review. *Oral Dis*. 2021;27:27–41.
27. Schubert O, Schweiger J, Stimmelmayr M, Nold E, Güth JF. Digital implant planning and guided implant surgery—workflow and reliability. *Br Dent J*. 2019;226:101–108.
28. Ishak MI, Kadir MR, Sulaiman E, Kasim NH. Finite element analysis of zygomatic implants in intrasinus and extramaxillary approaches for prosthetic rehabilitation in severely atrophic maxillae. *Int J Oral Maxillofac Implants*. 2013;28: e151–160.
29. Varghese KG, Kurian N, Gandhi N, et al. Three-dimensional finite element analysis of zygomatic implants for rehabilitation of patients with a severely atrophic maxilla. *J Prosthet Dent*. 2023;129:597.e591–597.e598.
30. Lee SJ, Jamjoom FZ, Le T, Radics A, Gallucci GO. A clinical study comparing digital scanning and conventional impression making for implant-supported prostheses: a crossover clinical trial. *J Prosthet Dent*. 2022;128:42–48.
31. Revilla-León M, Att W, Özcan M, Rubenstein J. Comparison of conventional, photogrammetry, and intraoral scanning accuracy of complete-arch implant impression procedures evaluated with a coordinate measuring machine. *J Prosthet Dent*. 2021;125:470–478.
32. Ma B, Yue X, Sun Y, Peng L, Geng W. Accuracy of photogrammetry, intraoral scanning, and conventional impression techniques for complete-arch implant rehabilitation: an in vitro comparative study. *BMC Oral Health*. 2021; 21:636.